Fully Polarimetric SAR Image Filtering by Combining Block Matching and Lee Filter

Guisheng Zhao, Shengyuan Zhu, and Yinglei Wu

***Abstract*—Speckle filtering is a key preprocessing approach for the applications of polarimetric synthetic aperture radar (PolSAR) data. Most current PolSAR filtering algorithms can hardly get good balance in suppressing speckle and retaining image details. In this article, an algorithm for fully PolSAR image filtering is proposed by embedding the idea of the advanced block matching theory into the classical Lee filter, which ensures that image details can be well preserved after the significant reduction of speckle. First, taking each image block as the reference, a block matching step is taken to group those similar blocks in the nonlocal area; the Lee filter is employed to simultaneously process the center pixel of each block in the group, followed by an aggregation step which estimates the same pixel been grouped in different groups; then, the block matching step is taken again to regroup similar blocks by using the information of both the original image and the image filtered in last stage; again, the Lee filter is collaborated with the aggregation step in filtering the image. Despeckling experiments demonstrate that the proposed PolSAR filter can not only significantly suppress the image noise but also well preserve edges and textures.**

***Index Terms*—Block matching, nonlocal, speckle, synthetic aperture radar.**

I. Introduction

NOWADAYS, the fully polarimetric SAR remote sensing technique has attracted wide attention, due to its advantages in observing the land objects in different weather conditions and providing more backscattering information. More and more commercial polarimetric synthetic aperture Radar (PolSAR) satellites have been launched in the last decade, making PolSAR data easier to be accessed and facilitating the various applications of PolSAR data [1], [2], [3]. However, SAR sensors can encounter some image degradation issues. Among them, speckle noise is a non-negligible problem, which seriously complicates most image interpretation works [4]. Undoubtedly, it is imperative to develop speckle filtering method.

Among all the PolSAR filters presented in the last three decades, the Lee filter [5] is one of the most widely used methods, since it is easy to be operated, robust, and with high processing efficiency. In the Lee filter, each target pixel is filtered by the pixel intensity values of the local filtering window centered at the target pixel, based on the principle of minimum mean square error (MMSE). The main drawbacks of the original Lee filter can be concluded as two aspects [6], [7]: on one hand, the pixels in the local filtering window can be highly dissimilar in the image areas with rich textures, making the basic assumption of local homogeneity in the MMSE estimator not stand; on the other hand, since the Lee filter is a kind of statistical based filter, small local window with very limit number of pixels can bring bias in estimating the parameters in the filter. Some studies have been done by researchers to solve the above-mentioned drawbacks and to improve the Lee filter [8], [9], [10], [11]. The strategies taken in these studies are mainly to enlarge the filtering window and to search similar pixels with regard to the target pixel before filtering. In a sense, all the aforementioned methods belong to the local filters.

The idea of nonlocal filtering, originally developed for optical image denoising [12], has also been used in the field of PolSAR image despeckling [13], [14], [15]. In the nonlocal filters, the similarity between two pixels is obtained not by comparing the values of themselves as did in the local filters but by comparing the image blocks centered at them. By doing so, the information on image structures can be considered, and hence this information can be better retained after filtering.

The framework of nonlocal filtering inspired us with the idea to mitigate the drawbacks of the classical Lee filter and take full advantage of nonlocal filtering: by matching and grouping those similar image blocks in a large nonlocal area, the target pixels can be filtered by the PolSAR Lee filter with more pixels and with more accurate parameters. Based on this idea, a PolSAR filtering method embedding the block matching strategy into the Lee filter is proposed in this article, which consists of two stages, namely the initial estimation stage and the final estimation stage, and each stage includes the block matching, the filtering, and the aggregation steps. In the initial estimation stage, a block matching step is taken to group those similar blocks for each reference block, the Lee filter is employed to simultaneously process the center pixel of each block in the group, and an aggregation approach is employed to estimate the same pixel been grouped in different groups. The process of the final estimation stage is similar to that of the initial estimation stage, with the difference that the block matching step and the Lee filter consider the information of both the original data and the initially estimated data.

Manuscript received 28 November 2023; revised 10 February 2024 and 4 April 2024; accepted 24 May 2024. Date of publication 29 May 2024; date of current version 14 June 2024. This work was supported by the Hefei Municipal Natural Science Foundation under Grant 2021142. *(Corresponding author: Guisheng Zhao.)*

Guisheng Zhao is with the Hefei Construction Quality and Safety Supervision Station, Hefei 230061, China (e-mail: zguisheng@foxmail.com).

Shengyuan Zhu and Yinglei Wu are with the China JIKAN Research Institute of Engineering Investigations and Design, Company Ltd., Xi'an 230012, China (e-mail: zhusy@jk.com.cn; wuyinglei1013@163.com).

Digital Object Identifier 10.1109/JSTARS.2024.3406751

It must be pointed out that Zhong et al. [16] proposed a PolSAR filter named the Distributive NL-Lee (DNL-Lee) filter which also combines the Lee filter and the idea of nonlocal. However, distinguished differences exist between the proposed filter and the DNL-Lee filter. In the DNL-Lee filter, a kind of hybrid patch similarity measure is constructed by combining together the structure similarity introduced by the nonlocal means filter and the homogeneity similarity introduced by the Lee filter, which works in a distributive way. That is to say, the emphasis of the work in [16] is how to select similar pixels by considering both the structure similarity and the homogeneity similarity. Compared with the DNL-Lee filter, the proposed filter not only considers the structure similarity (in the block matching step) and the homogeneity similarity (in the estimation step), but also can get multiple estimations for each pixel in different groups (in the aggregation step), thus reducing bias of the estimation of a pixel in a certain group.

The rest of this article is organized as follows. First, we recall the statistical straits of speckle and the PolSAR Lee filter in Section II. Then, the Block Matching based Lee (BM-Lee) filter is proposed in Section III, the performance of which is validated by the despeckling results provided in Section IV. The discussion is made in Section V. Finally, we conclude this article in Section VI.

II. Related Works

The speckled SAR intensity data have the multiplicative nature, which can be modeled as follows:

$$I = n \cdot u \tag{1}$$

where I is the contaminated SAR intensity image, n represents the noise component, and u is the unobserved clean data. The Lee filter [5] assumes that the filtered data I' and the prior mean $\overline{I}$ calculated by the mean value of all pixels in the filtering window have the following linear relationship:

$$I' = \overline{I} + \alpha(I - \overline{I}) \tag{2}$$

where the parameter α plays a role in balancing the weights of the speckled data and the prior mean. In a homogeneous filtering window, α should be close to 0, such that the filtered value of the center pixel is close to the prior mean to ensure significant reduction of speckle. In a highly heterogeneous filtering window with rich edges and structures, α should be close to 1, such that the center pixel keeps unfiltered to preserve image details.

Based on the principle of MMSE, the parameter a is derived as follows:

$$\alpha = \frac{\mathrm{var}(I) - \overline{I}/L}{(1 + 1/L^2)\mathrm{var}(I)} \tag{3}$$

where $\mathrm{var}(\cdot)$ denotes the variance of the pixel values, and L is the number of looks.

Compared with the statistical traits of speckle in SAR intensity data, the statistical traits of speckle in fully PolSAR data are more complex, since the diagonal elements of polarimetric covariance matrix (PCM) are contaminated by multiplicative noise, while the other elements are contaminated by mixed noise [17]. Early PolSAR filtering methods processed the different elements of PCM separately, which introduced unwanted crosstalk between different polarization states [18], [19]. To avoid this problem, Lee et al. [4] proposed to extend and refine the original Lee filter to process PolSAR data in the following form:

$$\boldsymbol{C}' = \bar{\boldsymbol{C}} + \alpha(\boldsymbol{C} - \bar{\boldsymbol{C}}) \tag{4}$$

where $\boldsymbol{C}$ is the speckled PCM, $\bar{\boldsymbol{C}}$ is the local mean of $\boldsymbol{C}$, and α is calculated using the intensity data as in the original Lee filter. Different from the original Lee filter with square filtering window, edge-aligned nonsquare filtering window is used in the PolSAR Lee filter.

III. Block Matching Based Lee Filter

In this section, we propose the BM-Lee filter, the main idea of which is to research similar blocks in a nonlocal area and to refine the estimation results of the classical Lee filter. The BM-Lee filter consists of the initial estimation stage and the final estimation stage. Each stage includes the block matching, the filtering, and the aggregation steps. The basic scheme of the BM-Lee filter is displayed in Fig. 1.

A. Similarity Measure Between PolSAR Image Blocks

For the proposed filter which employs the idea of nonlocal means, the similarity measure between PolSAR image blocks is a key issue that should be considered in the block matching steps.

Some algorithms have been presented in literatures to measure the similarity between PolSAR image blocks [20], [21]. Among them, the likelihood ratio test (LRT) similarity [20] and the Kullback–Leibler divergence (KLD) similarity [21] show good performances. By comparing the similarity between each two corresponding pixels in the same position of two images block and taking average of the pixel similarity values, the similarity between blocks is obtained.

The LRT similarity was derived from the fact that the speckled PCM follows a Wishart distribution [22]. Let two matrices X_1 and Y_1 follow the same Wishart distribution, the LRT similarity between them is as follows:

$$S_{\mathrm{SRT}}(X_1, Y_1) = 6 \ln 2 + \ln|X_1| + \ln|Y_1| - 2\ln|X_1 + Y_1| \tag{5}$$

where ln denotes the natural logarithm and $|\cdot|$ is the determinant. The value range of S_1 is $(-\infty, 0]$ and S_1 equals to 0 if X equals to Y.

Compared with the LRT similarity, the KLD similarity was developed without relying on assumptions of the statistical traits of PCM, and hence it is more suitable for the similarity measure for the image after filtering. The LRT similarity between two matrices X_2 and Y_2 is

$$S_{\mathrm{KLD}}(X_2, Y_2) = \mathrm{tr}(X_2^{-1} \cdot Y_2) + \mathrm{tr}(X_2 \cdot Y_2^{-1}) - 6 \tag{6}$$

where $\mathrm{tr}(\cdot)$ represents the trace of PCM.

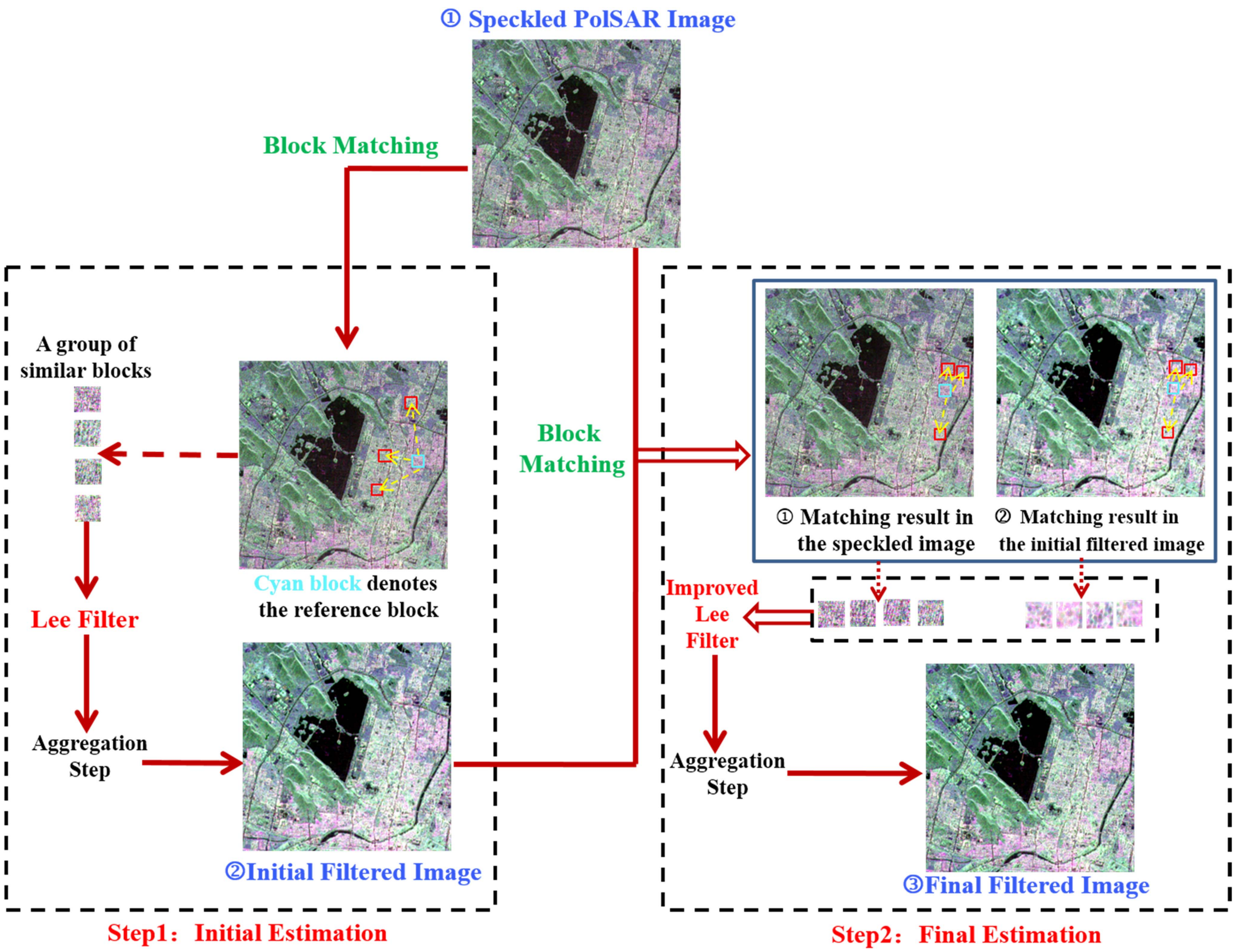

Fig. 1. Diagram of the proposed BM-Lee filter.

B. Initial Estimation Stage

In this stage, we employ the LRT similarity to match similar blocks in the speckled image, since it well exploits the statistical traits of the speckled data. We used 3×3 blocks to ensure better edge-preservation results and save computational time. For the similarity threshold, we found that -20 is an appropriate value through a number of experiments.

For each reference block (the image patch centered at each pixel), all the similar blocks in its nonlocal areas are found and the center pixels of these blocks are grouped together by the above-mentioned block matching step. Then, the Lee filter [see (2)] is used to simultaneously process all pixels in the group.

It must be noted that, during the grouping process, any pixel in a certain position of the image could be placed into different groups. That is to say, we may get multiple estimation values for the same pixel. Therefore, we need to aggregate the multiple estimations of the same pixel, assign weights for the different estimations, and take a weighted average of the multiple estimations to get the filtering image of this stage. In this study, we set the weights by considering the traits of the parameter α in the Lee filter. It can be seen that the parameter αmeasures the homogeneity of each group. A low α value indicates that the pixels in a group are quite similar, and in theory, the estimation results by the Lee filter are more accurate. Therefore, the weight for the ith estimation of a certain pixel is set as follows:

$$W_i = (1-\alpha_i)/\sum_{j=1}^{N}(1-\alpha_j) \tag{7}$$

where N denotes the number of estimations.

C. Final Estimation Stage

The procedure of the final estimation stage is similar to that of the initial estimation stage, but differences exist in the similarity measure of the BM step and in the filtering step.

In the BM step, the similarity between blocks is measured by considering the information of both the speckled and initially estimated data, such that the similar blocks can be grouped more accurately. The new similarity measure for two blocks centered at pixels i and j is

$$S = S_{\mathrm{LRT}}(\boldsymbol{C}(i), \boldsymbol{C}(j)) \cdot S_{\mathrm{KLD}}(\boldsymbol{C}_o(i), \boldsymbol{C}_o(j)) \tag{8}$$

where $\boldsymbol{C}$ and $\boldsymbol{C}_o$ are, respectively, the PCMs of a block in the speckled and initially filtered images. We use the KLD similarity to measure the similarity of the initial estimation because the PolSAR data after processing does not follow the Wishart distribution. Given a reference block, through the above-mentioned BM step, two-pixel groups are formed: one is from the speckled image, the other one is from the initial filtered image, and the pixels in both of them are located in the same positions. Different from the similarity threshold in the initial estimation step, we found that the optimal similarity threshold in the final estimation step is not fixed. By conducting a number of experiments, we found that the threshold is generally proportional to the number of looks, and it is about $-15L$.

In the filtering step, since we have the initial estimations, we can use them to refine the calculation of the prior mean in the Lee filter [see (2) and (3)]. Thus, the prior mean of pixels in a group is calculated by their mean value in the initial estimated image

IV. Experimental Part

In this section, PolSAR despeckling experiments on a simulated image and two images acquired by GF-3 satellite are reported to inspect the performances of the BM-Lee filter. The performances of the refined PolSAR Lee filter [4], the PolSAR nonlocal means proposed by Chen et al. [15], and the DNL-Lee filter [16] are also reported for comparison.

A. Experiments on Simulated Image

In this part, we employed the Monte Carlo approach [23] to generate a single-look PolSAR image. To quantify the filtering performances of the different algorithms, two indicators, namely the equivalent number of looks (ENL) [24] and the edge-preservation degree based on the ratio of average (EPD-ROA) [25], are used.

ENL can be calculated by

$$\mathrm{ENL} = 1/\sigma^2 \tag{9}$$

where σ represents the coefficient of variation of the signal values in homogeneous areas.

EPD-ROA is defined as follows:

$$\mathrm{EPD-ROA} = \frac{\sum_{i=1}^{m} |I'_1(i)/I'_2(i)|}{\sum_{i=1}^{m} |I_1(i)/I_2(i)|} \tag{10}$$

where m is the total pixel number; I' and I denote the despeckled and the original speckled intensity images, respectively; the subscripts denote two neighboring pixels. The value range of EPD-ROA is between 0 and 1, and in theory, the EPD-ROA value for a filter well retained the edges is close to 1.

Fig. 2 shows the filtering results on the simulated PolSAR image. The images are the Pauli RGB images, which are formed with intensities of $|S_{HH} - S_{VV}|$ (red), $|S_{HV} + S_{VH}|$ (green), and $|S_{HH} + S_{VV}|$ (blue). It can be observed that the refined Lee filter suppresses the speckle to some degree, but some unwanted block effects appear in homogeneous areas; besides, the boundaries between different areas are blurred. The nonlocal means significantly reduce the speckle, but some edges and small targets are not well retained. The DNL-Lee filter shows better performances in retaining edges and small targets, but the spatial resolution of the filtered image slightly degrades. Generally speaking, the BM-Lee filter makes a good compromise between suppressing noise and retaining image details. The assessment values listed in Table I support the above-mentioned observations that the BM-Lee filter not only suppresses the speckle to a large degree but also retains most image details.

TABLE I
Quantitative Assessments on the Simulated Image

	ENL	EPD-ROA
Refined Lee	31.2	0.66
Nonlocal Means	60.1	0.79
DNL-Lee	62.4	0.82
BM-Lee	56.7	0.91

TABLE II
Quantitative Assessments on the GF-3 Images

		Refined Lee	Nonlocal Means	DNL-Lee	BM-Lee
GF-3 QPSI image	**ENL**	22.0	31.4	29.9	29.6
	EPD-ROA	0.57	0.62	0.63	0.66
GF-3 QPSII image	**ENL**	24.4	33.7	35.1	27.8
	EPD-ROA	0.65	0.60	0.58	0.71

B. Experiments on GF-3 Images

The first image was acquired by GF-3 satellite working in the quad-polarimetric strip I (QPSI) mode with a resolution of 8 m. As shown in Fig. 3, the scene in this image is relatively complicated, since it contains several typical kinds of land object. For example, the water is dominated by odd scattering mechanism, the forests are dominated by volume scattering mechanism, and the build-up areas with complex scattering mechanisms. As observed, the refined Lee filter still shows the block effect because the edge-aligned filtering window is used instead of the normal square window, leading to the problem of smearing image details, which is exhibited in the ratio image between the speckled data and the filtered data. Again, the nonlocal means filter significantly reduces the speckle and shows better edge retention results. However, the oversmoothing issue still exists. The DNL-Lee filter performs better in retaining image details and also well suppresses the speckle. From Fig. 3 and the assessments in Table II, it is apparent that, compared with the other three filters, the BM-Lee filter obtains a satisfactory balance between reducing noise and retaining the spatial resolution of the image.

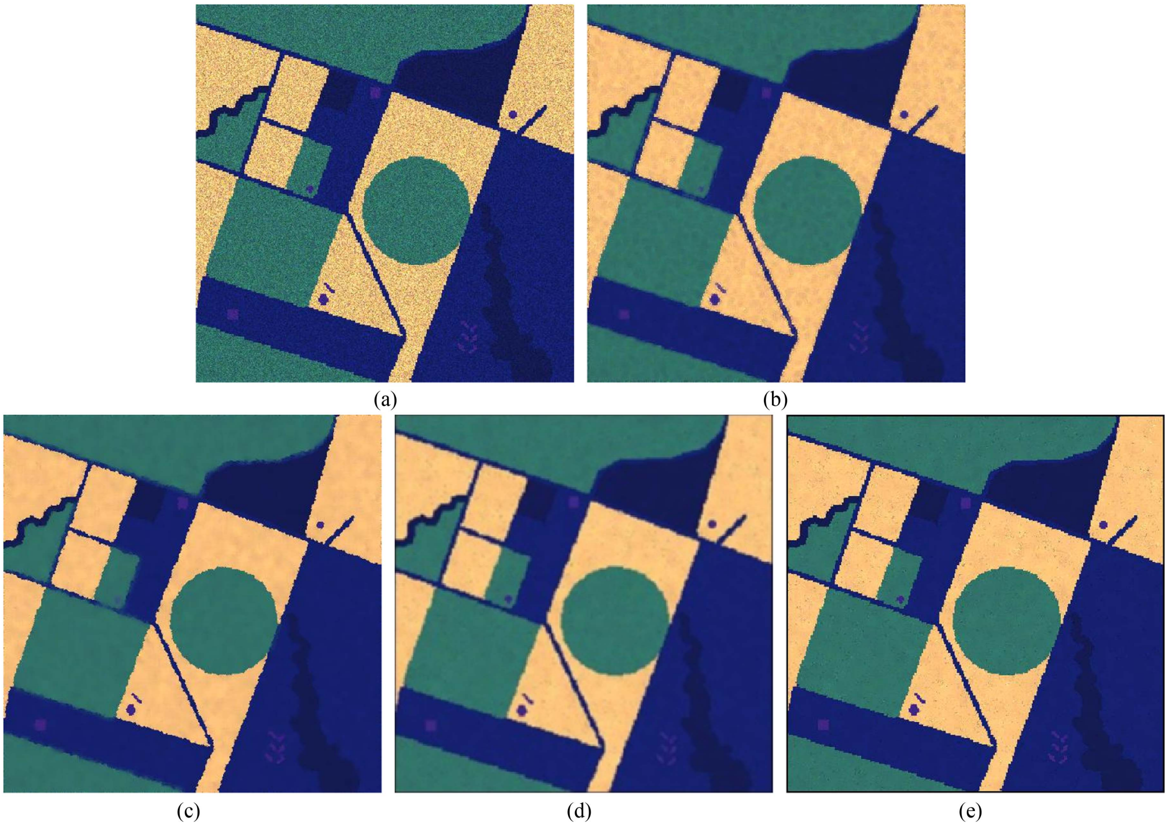

Fig. 2. Experimental results on the simulated image. (a) Single-look Pauli RGB image. (b)–(e) Pauli RGB images despeckled by the refined Lee filter, the nonlocal means, the DNL-Lee filter, and the BM-Lee filter, respectively.

Noise exists in PolSAR images makes the different types of land objects difficult to be distinguished. A satisfactory filtering method should make land objects more distinguishable by reducing the speckle and preserving the scattering mechanisms of objects. To inspect this issue, we chose three areas in the image from the water area, the forest area, and the urban area, respectively, and obtained the Cloude polarimetric decomposition parameters [26] (i.e., entropy H, anisotropy A, and scattering angle α) for all pixels in these areas. Then, we plotted the scattergrams of these pixels in the $H/A/\alpha$ space, as shown in Fig. 4. It can be observed that, compared with the sparsely distributed scatters in the original image influenced by speckle, the scatters in the filtered images become much more concentrated due to the suppression of speckle, especially for the water pixels and the forest pixels. Besides, it can be noticed that, for the DNL-Lee and BM-Lee filtered image, the scatters of water and forest are highly concentrated while some scatters of building are still sparsely distributed. The reason is that, compared with the water and forest areas, the scene and scattering mechanisms of the urban area are much more complicated, and the DNL-Lee and BM-Lee filters not only reduce the speckle in homogeneous areas but also effectively preserve the complicated scattering mechanisms of targets.

The second image was acquired by GF-3 satellite working in the quad-polarimetric strip II (QPSII) mode. As displayed in Fig. 5 and Table II, once again, the refined Lee filtered result is not satisfactory due to the appearance of block effect and the smearing of image. Over smoothing problem exists in the nonlocal means and DNL-Lee filtered images. As expected, a better filtering result is obtained by the proposed BM-Lee filter.

V. Discussion

In the estimation step of the proposed method, the MMSE estimator (i.e., the Lee filter) is used. The key of effectively applying the Lee filter is to ensure the homogeneity of pixels which participate in the filtering process since this filter is derived based on the assumption of multiplicative noise. Based on the above-mentioned fact, some filters have been proposed to improve the Lee filter. For example, the refined Lee filter [4] used an edge-aligned window to select similar pixels, but only considering the intensity similarity and using the small local window with very limit number of pixels which can bring bias in estimating the parameter in the filter; the IDAN filter [9] expands the filtering window and uses adaptive strategy to choose similar pixels, but still only consider intensity similarity; the scattering-model-based filter [8] finds similar pixels in local window by considering polarimetric scattering mechanisms. In all the aforementioned studies, the researchers have found and agreed the basic conclusion that, if a larger number of very similar pixels are chosen in the filtering process, the performance of the MMSE filter can be improved. That is the basic start point

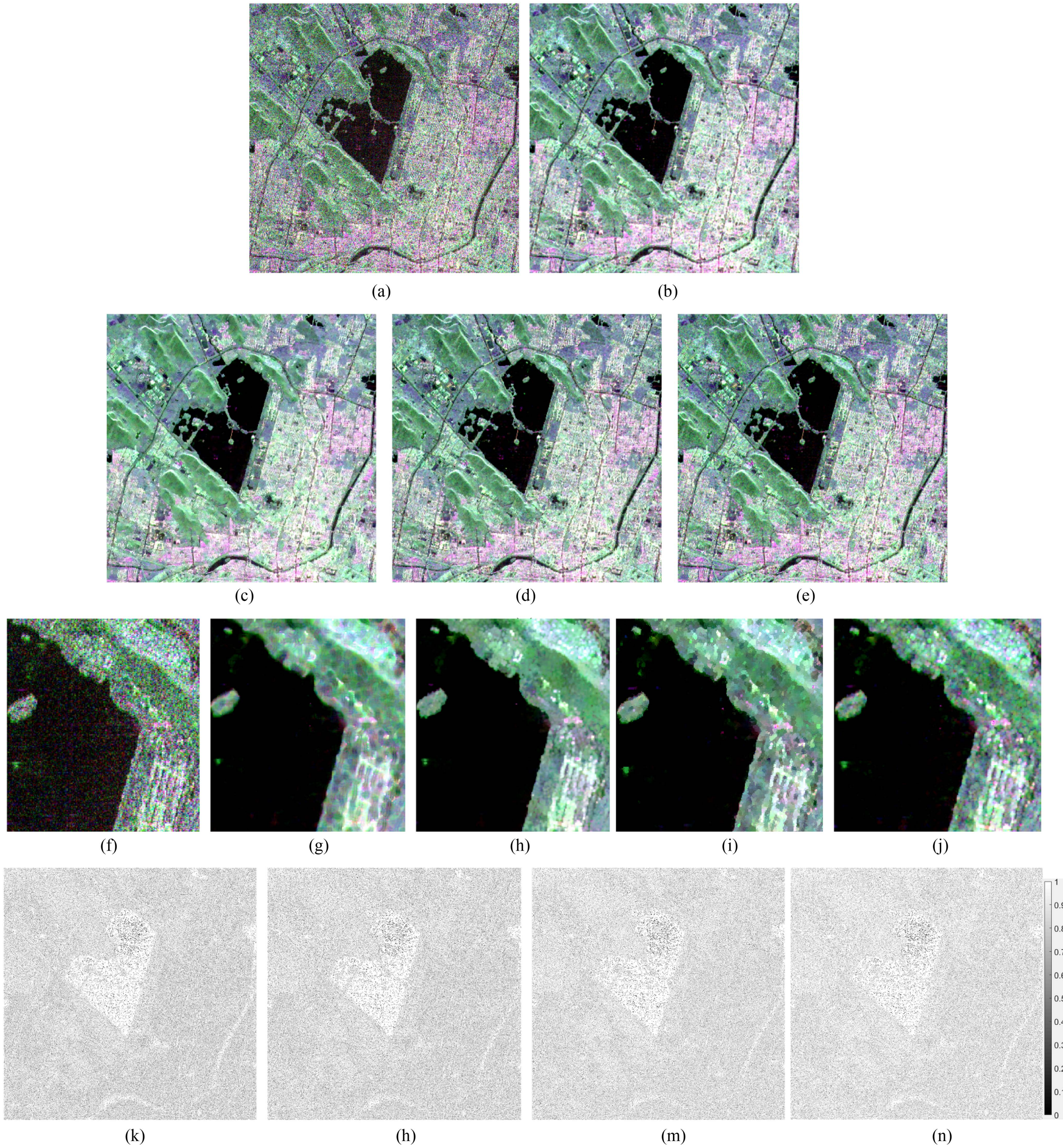

Fig. 3. Experiments on GF-3 QPSI image. (a) Original Pauli RGB image. (b)–(e) Pauli RGB images despeckled by the refined Lee filter, the nonlocal means, the DNL-Lee filter, and the BM-Lee filter, respectively. (f)–(j) Subimages cropped from (a) to(e), respectively. (k)–(n) Ratio image of (b)–(e), respectively.

of our study which uses the idea of nonlocal (especially the 3D patch matching idea) to keep the homogeneity of pixels that participate in the filtering process.

To inspect the validity of employing the MMSE filter in the estimation step of the proposed method, we display the map for the values of parameter α calculated on the GF-3 QPSI image [Fig. 6(b)]. As can be seen, the α values are generally in line with the real state that, in those areas with less textures, such as forest and water areas, the values are lower (close to 0), while in those areas with complicated textures, such as urban areas, the values are higher (close to 1).

We also display a filtered image of the method which replaces the MMSE filter by mean filter (i.e., a special case that parameter α is fixed as 0) in Fig. 6. It can be clearly observed that, compared with the proposed method with MMSE filter, the method with mean filter shows notable oversmoothing problem, which means

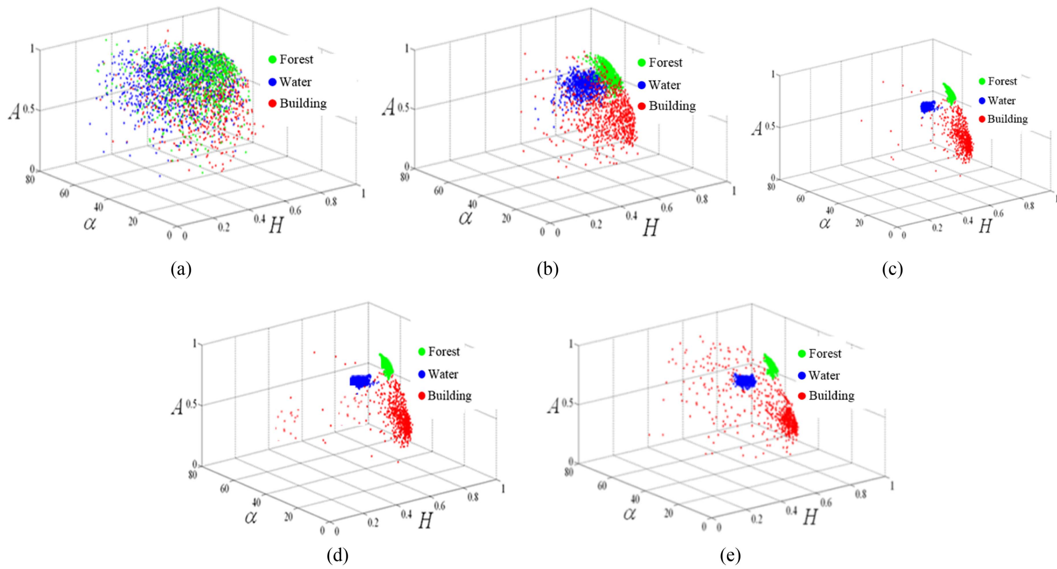

Fig. 4. Scattergrams of pixels in the *H*/*A*/α space. (a)–(e) Scattergrams for the original data, the refined Lee filtered data, the nonlocal mean filtered data, the DNL-Lee filtered, and the BM-Lee filtered data, respectively.

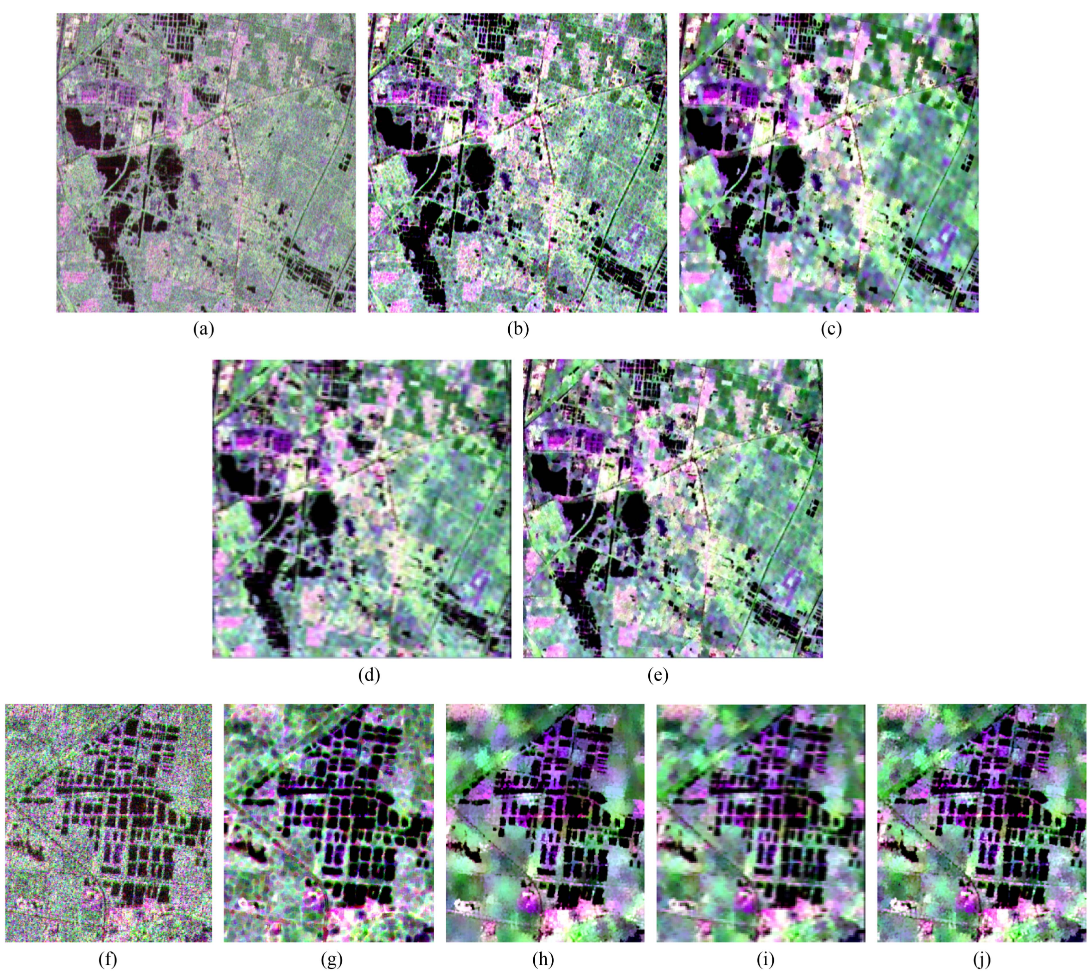

Fig. 5. Experiments on GF-3 QPSII image. (a) Original Pauli RGB image. (b)–(e) Pauli RGB images despeckled by the refined Lee filter, the nonlocal means, the DNL-Lee filter, and the BM-Lee filter, respectively. (f)–(j) Subimages cropped from (a) to (d), respectively.

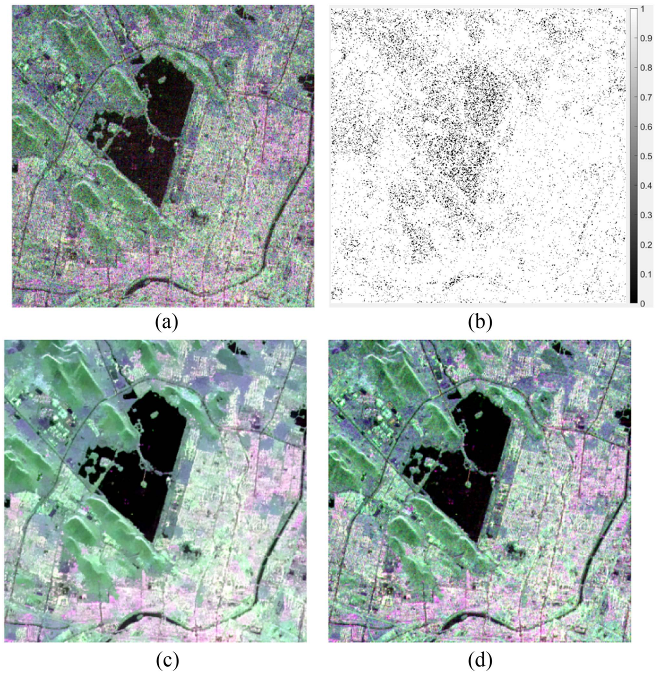

Fig. 6. Experiments on GF-3 QPSI image. (a) Original image. (b) Values of parameter α. (c) and (d) Images despeckled by the proposed method with mean filter and MMSE filter, respectively.

that employing the adaptive MMSE filter in the estimation step of the proposed method can indeed improve the filtering performance.

VI. Conclusion

Fully polarimetric SAR image despeckling is a meaningful but challenging work. The traits of speckle in fully PolSAR data are much more complicated than those in SAR data in intensity format or in amplitude format. Most current PolSAR filtering algorithms can hardly get good balance in suppressing speckle and retaining image details. In this article, a PolSAR filtering method named BM-Lee filter is proposed, by combining the idea of the advanced block matching theory with the classical Lee filter, with the aim of retaining image details while significantly reducing speckle. The proposed filter consists of the initial estimation stage and the final estimation stage, and the estimation results in the initial stage are used to refine the final estimations. Each stage includes the block matching, the filtering, and the aggregation steps. Despeckling experiments validate that the proposed PolSAR filter can not only notably filter out the image noise but also well retain edges and textures. However, it must be noted that, since block matching strategy is employed, the processing speed of the proposed filter is relatively slow. Therefore, our future work will focus on accelerating the algorithm. It should be noted that, as revealed in some studies [15], [27], for a certain nonlocal filter, image details tend to be better retained if small sizes of image patch and search neighborhood are used, while noise tends to be better suppressed if large sizes are used. Therefore, in theory, an adaptive strategy to choose the optimal patch size and search neighborhood size is helpful for the nonlocal filter to get a good balance between edge preservation and noise reduction. The proposed filter in this study fixed the patch size and search neighborhood size. In our future work, we will study the topic of improving the proposed filter by automatically selecting optimal sizes of image patch and search neighborhood.

References

[1] X. S. Ma, J. G. Xu, J. Pan, J. Yang, and X. C. Meng, "Detection of marine oil spills from radar satellite images for the coastal ecological risk assessment," *J. Environ. Manage.*, vol. 325, Jan. 2023, Art. no. 116637.

[2] K. Lasko, K. Vadrevu, and V. Tran, "Mapping double and single crop paddy rice with Sentinel-1A at varying spatial scales and polarizations in Hanoi, Vietnam," *IEEE J. Sel. Topics Appl. Earth Observ. Remote Sens.*, vol. 11, no. 2, pp. 498–512, Feb. 2018.

[3] S. Kobayashi and H. Ide, "Rice crop monitoring using Sentinel-1 SAR data: A case study in Saku, Japan," *Remote Sens.*, vol. 14, no. 14, pp. 3254–3274, Jul. 2022.

[4] J. S. Lee, M. Grunes, and G. De Grandi, "Polarimetric SAR speckle filtering and its implication for classification," *IEEE Trans. Geosci. Remote Sens.*, vol. 37, no. 5, pp. 2363–2373, Sep. 1999.

[5] J. S. Lee, "Digital image enhancement and noise filtering by use of local statistics," *IEEE Trans. Pattern Anal. Mach. Intell.*, vol. 2, no. 2, pp. 165–168, Mar. 1980.

[6] Y. Shen, X. Ma, S. Zhu, and J. Xu, "Polarimetric SAR speckle filtering using a nonlocal weighted LMMSE filter," *Sensors*, vol. 21, no. 21, Nov. 2021, Art. no. 7393.

[7] X. Ma, C. Wang, and Z. Yin, "SAR image despeckling by noisy reference-based deep learning method," *IEEE Trans. Geosci. Remote Sens.*, vol. 58, no. 12, pp. 8807–8818, Dec. 2020.

[8] J. S. Lee, M. Grunes, D. Schuler, E. Pottier, and L. Ferro-Famil, "Scattering-model-based speckle filtering of polarimetric SAR data," *IEEE Trans. Geosci. Remote Sens.*, vol. 44, no. 1, pp. 176–187, Jan. 2006.

[9] G. Vasile, E. Trouve, J. S. Lee, and V. Buzuloiu, "Intensity-driven adaptive-neighborhood technique for polarimetric and interferometric SAR parameters estimation," *IEEE Trans. Geosci. Remote Sens.*, vol. 44, no. 6, pp. 1609–1621, Jun. 2006.

[10] J. S. Lee, J. H. Wen, T. L. Ainsworth, K. S. Chen, and A. J. Chen, "Improved sigma filter for speckle filtering of SAR imagery," *IEEE Trans. Geosci. Remote Sens.*, vol. 47, no. 1, pp. 202–213, Jan. 2009.

[11] Z. Ding, T. Zeng, F. Dong, L. Liu, W. Yang, and T. Long, "An improved PolSAR image speckle reduction algorithm based on structural judgment and hybrid four-component polarimetric decomposition," *IEEE Trans. Geosci. Remote Sens.*, vol. 51, no. 8, pp. 4438–4449, Aug. 2013.

[12] A. Buades, B. Coll, and J. M. Morel, "A non-local algorithm for image denoising," in *Proc. IEEE Comput. Soc. Conf. Comput. Vis. Pattern Recognit.*, Jun. 2005, pp. 60–65.

[13] C. Wang, Z. Yin, X. Ma, and Z. Yang, "SAR image despeckling based on block-matching and noise-referenced deep learning method," *Remote Sens.*, vol. 14, 2022, Art. no. 391.

[14] S. Parrilli, M. Poderico, C. V. Angelino, and L. Verdoliva, "A nonlocal SAR image denoising algorithm based on LLMMSE wavelet shrinkage," *IEEE Trans. Geosci. Remote Sens.*, vol. 50, no. 2, pp. 606–616, Feb. 2012.

[15] J. Chen, Y. Chen, W. An, Y. Cui, and J. Yang, "Nonlocal filtering for polarimetric SAR Data: A pretest approach," *IEEE Trans. Geosci. Remote Sens.*, vol. 49, no. 5, pp. 1744–17543, May 2011.

[16] H. Zhong, J. Zhang, and G. Liu, "Robust polarimetric SAR despeckling based on nonlocal means and distributed Lee filter," *IEEE Trans. Geosci. Remote Sens.*, vol. 52, no. 7, pp. 4198–4210, Jul. 2014.

[17] J. S. Lee and E. Pottier, *Polarimetric Radar Imaging: From Basics to Applications*, vol. 33. Boca Raton, FL, USA: CRC Press, Feb. 2009, pp. 661–662.

[18] L. M. Novak and M. C. Burl, "Optimal speckle reduction in polarimetric SAR imagery," *IEEE Trans. Aerosp. Electron. Syst.*, vol. 26, no. 2, pp. 293–305, Mar. 1990.

[19] A. Lopes and F. Sery, "Optimal speckle reduction for the product model in multilook polarimetric SAR imagery and the Wishart distribution," *IEEE Trans. Geosci. Remote Sens.*, vol. 35, no. 3, pp. 632–647, May 1997.

[20] K. Conradsen, A. A. Nielsen, J. Schou, and H. Skriver, "A test statistic in the complex Wishart distribution and its application to change detection in polarimetric SAR data," *IEEE Trans. Geosci. Remote Sens.*, vol. 41, no. 1, pp. 4–19, Jan. 2003.

[21] O. D. Hondt, S. Guillaso, and O. Hellwich, “Iterative bilateral filtering of polarimetric SAR data,” *IEEE J. Sel. Topics Appl. Earth Observ. Remote Sens.*, vol. 6, no. 3, pp. 1628–1639, Jun. 2013.

[22] N. R. Goodman, “Statistical analysis based on a certain multivariate complex Gaussian distribution (An introduction),” *Ann. Math. Statist.*, vol. 34, no. 1, pp. 152–177, Mar. 1963.

[23] J. S. Lee, M. R. Grunes, and R. Kwok, “Classification of multi look polarimetric SAR imagery based on complex Wishart distribution,” *Int. J. Remote Sens.*, vol. 15, no. 11, pp. 2299–2311, Aug. 1994.

[24] A. Lopes, R. Touzi, and E. Nezry, “Adaptive speckle filters and scene heterogeneity,” *IEEE Trans. Geosci. Remote Sens.*, vol. 28, no. 6, pp. 992–1000, Nov. 1990.

[25] H. Feng, B. Hou, and M. Gong, “SAR image despeckling based on local homogeneous-region segmentation by using pixel-relativity measurement,” *IEEE Trans. Geosci. Remote Sens.*, vol. 49, no. 7, pp. 2724–2737, Jul. 2011.

[26] S. Cloude and E. Pottier, “An entropy based classification scheme for land applications of polarimetric SAR,” *IEEE Trans. Geosci. Remote Sens.*, vol. 35, no. 1, pp. 68–78, Jan. 1997.

[27] C. A. Deledalle, L. Denis, F. Tupin, A. Reigber, and M. Jäger, “NL-SAR: A unified nonlocal framework for resolution-preserving (Pol)(In)SAR denoising,” *IEEE Trans. Geosci. Remote Sens.*, vol. 53, no. 4, pp. 2021–2038, Apr. 2015.

Guisheng Zhao received the B.S. degree in industrial and civil architecture from Anhui Jianzhu University, Hefei, China, in 2008.

He is currently a Senior Engineer with Hefei Construction Quality and Safety Supervision Station, Hefei, China. His research interests include photogrammetry, remote sensing, and engineering survey.

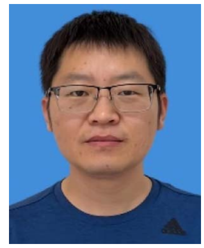

Shengyuan Zhu received the B.S. degree in surveying and mapping engineering from China University of Mining and Technology, Xuzhou, China, in 2008.

He is currently a Senior Engineer with China JIKAN Research Institute of Engineering Investigations and Design, Company Ltd., Xi’an, China. His research interests include remote sensing image processing, application of remote sensing data, and engineering survey.

Yinglei Wu received the B.S. degree in surveying and mapping engineering from the Hebei University of Engineering, Handan, China, in 2012, and the master’s degree in surveying and mapping engineering from Hefei University of Technology, Hefei, China, in 2015.

He is currently an Engineer with China JIKAN Research Institute of Engineering Investigations and Design, Company Ltd., Xi’an, China. His research interests include application of remote sensing data and engineering survey.